GPS Solutions (2020) 24:52
https://doi.org/10.1007/s10291-020-0966-4

ORIGINAL ARTICLE

Triple-frequency multi-GNSS reflectometry snow depth retrieval by using clustering and normalization algorithm to compensate terrain variation

Zhiyu Zhang[1] · Fei Guo[1,2] · Xiaohong Zhang[1,2]

Received: 16 May 2019 / Accepted: 26 February 2020 / Published online: 4 March 2020

Abstract
Snow is an important water resource and plays a critical role in the hydrologic cycle. Accurate measurements of snow depth are needed by scientists to set up a more refined meteorology–hydrology model. Recently, the Global Navigation Satellite System Reflectometry (GNSS-R) has been developed and applied for snow depth monitoring, with low cost and high resolution. We propose an improved snow depth retrieval method using a combination of GNSS triple-frequency carrier phase. The topographic feature of the reflecting surface is considered for estimating the snow depth by using the density-based spatial clustering of applications with noise algorithm and normalization method. Observables from the GNSS station in Alaska, USA, are used to monitor snow depth and compared with the ground-truth measurements. Compared with the traditional triple-frequency snow depth retrieval method, the new approach has better performance for Galileo and BDS. The RMSE of the snow depth estimate reduces by nearly 40%, and the correlation coefficient increases from 0.93 to 0.97 for Galileo and from 0.91 to 0.95 for BDS, respectively. The research findings show no notable deviations on snow depth average estimation between Galileo and BDS observations compared to the GPS ones. Moreover, the solution with the proposed method results in improving spatial resolution due to the increasing number of satellites and better azimuth coverage.

Keywords Snow depth estimation · Global Navigation Satellite System Reflectometry (GNSS-R) · GNSS triple-frequency signals · Carrier phase combination

Introduction

The traditional ground-based snow monitoring techniques are limited by spatial and temporal sensitivity, while the snow depth measurements estimated by spaceborne passive microwave sensors are imprecise and costly (Larson et al. 2009; Qian and Jin 2016). Several investigations have demonstrated that Global Navigation Satellite System (GNSS) can be used as an L-band microwave radar for remote sensing purposes, such as tropospheric and ionospheric sounding, as well as earth's surface environments detection (Tabibi et al. 2015; Yu et al. 2018). Ground-based GNSS reflectometry (GNSS-R) is an emerging technique of environment sensing that can be used for monitoring near-surface parameters, such as snow depth and soil moisture (Rodriguez-Alvarez et al. 2011; Larson et al. 2008a; Chew et al. 2014; Alonso-Arroyo et al. 2014). The GNSS signals can provide many observations of snow depth from geodetic quality GNSS receivers of existing GNSS networks, with a sensing footprint size of about 1000 m^2 as an intermediate resolution falling between the in situ (< 1 m^2) and spaceborne (> 100 km^2) techniques (Larson 2016; Larson and Nievinski 2013).

Previous research (Bilich and Larson 2007; Nievinski and Larson 2014a; Larson et al. 2008b) has demonstrated that the amplitude and phase of multipath signals are in good agreement with the precipitation records and soil moisture retrieved by surrounding geodetic GNSS receiver. In parallel to the efforts in soil moisture retrievals, the surface snow depths were successfully estimated by using the frequency of the detrended signal-to-noise ratio (SNR) observables, which consist of direct and reflected components (Larson

✉ Fei Guo
fguo@whu.edu.cn

[1] School of Geodesy and Geomatics, Wuhan University, 129 Luoyu Road, Wuhan 430079, China

[2] Collaborative Innovation Center for Geospatial Technology, 129 Luoyu Road, Wuhan 430079, China

et al. 2009; Nievinski and Larson 2014c). Generally, the direct components can be removed from the SNR measurements by a low-order polynomial fitting, whereas the reflected components remain. Indeed, the SNR method can be independently applied to each carrier wave. The snow depth estimated by GPS L2C SNR measurements showed a great agreement with in situ snow depth (Larson et al. 2009). Moreover, the properties of snow depth retrieval using other signals have been investigated (Tabibi et al. 2015; Larson and Small 2016; Jin et al. 2016).

Since the SNR observables are not always available in the raw GNSS data file, Ozeki and Heki (2012) have proved that surface snow depth can be retrieved from a dual-frequency geometry-free linear combination (termed as L4 method) of the two L-band carriers GPS L1 and L2. Although the L4 method eliminates the influence of geometric parameters such as the satellite and receiver positions, the combination observables are degraded by inter-frequency ionospheric delays. So, the residual ionospheric delays must be removed by modeling as a high-order polynomial. Qian and Jin (2016) have extended the application of the L4 method to GLONASS, where the results have indicated that the estimation of the L4 method is comparable to the SNR method, and there is a good agreement between the estimations and the field reference values.

Recently, the latest generations of GNSS satellites such as modernized GPS (block IIF), Galileo and BDS are transmitting signals on three or more frequencies, thus having more choices in practice of snow depth retrieval. In order to simultaneously offset the effects of geometric factors and ionospheric delays, Yu et al. (2015) have proposed a triple-frequency phase combination by GPS L1/L2/L5 signals, which is free of geometry and ionospheric delays, to retrieve snow depth. The triple-frequency method performs significantly better than the L4 method and has similar performance as the SNR method.

Admittedly, the current data sets with triple-frequency carrier phases will, in general, also include high-quality SNR information. However, the performance of the SNR method largely depends on the successful removal of the direct components from the SNR measurements (Yu et al. 2018). As an alternative, the phase combinations contain only the interference terms and the sum of the integer ambiguities. Provided that there is no cycle slip in the raw phase observation, the sum of the integer ambiguities is a constant. Therefore, the triple-frequency combinations are not affected by the trend items caused by direct signal, which can avoid introducing the removal errors of the trend components, showing great potential in snow depth monitoring. Although the experimental results of the GPS triple-frequency method are encouraging, the snow depth estimation based on phase combination of BDS and Galileo signals needs further study. BDS and Galileo have longer revisit periods, and the ground tracks reappear at a more scattered azimuth. The variations of the track of sub-satellite points will introduce errors caused by terrain variation. In addition, since Galileo satellites transmit signals on five frequencies, i.e., E1, E5a, E5b, E5 and E6, there will be 10 different triple-frequency combinations. Therefore, the properties of different multipath phase combinations of Galileo need to be investigated to obtain the good performance of snow depth retrieval.

In this study, we propose an improved triple-frequency method to estimate snow depth, which is applicable to not only GPS but also BDS and Galileo systems. A clustering algorithm and normalization approach are applied to compensate for the effects of terrain variation caused by scattered observables. After the introduction, we present the principles and the problems of the traditional method and then introduce the proposed method. Following this, data collection and processing strategies are described. Thereafter, the performance evaluations of the proposed technique are shown. Eventually, the summarized conclusions are declared.

Traditional methods

Different from GPS, the variations of BDS and Galileo satellite track points will introduce errors caused by terrain variation due to their longer revisit periods. In this section, we first present the principles of snow depth retrieval with the triple-frequency combination. Then, the problems of the traditional triple-frequency method are pointed out.

Principles of the snow depth estimation with triple-frequency combination

The phase shift caused by interference of the direct and the reflected waves at the specular scattering point to the received mixed signal can be expressed as a function of satellite elevation angle, ε, and the vertical distance, H, from the reflection surface to antenna phase center (Elósegui et al. 1995),

$$\delta\phi(\varepsilon, H, \lambda) = \left(2\pi \frac{2H}{\lambda} \sin\varepsilon\right) \tag{1}$$

where λ is the carrier wavelength.

As shown in Fig. 1, when snow accumulates over the bare ground, the vertical distance from the horizontal reflector plane to the antenna phase center, H (Fig. 1a), will decrease to H' (Fig. 1b). If the antenna height of the land surface is known in advance, and the antenna height with snow-covered soil can be extracted from the multipath components of the signals, then the snow depth estimation, d, can be inferred from the variations of antenna height.

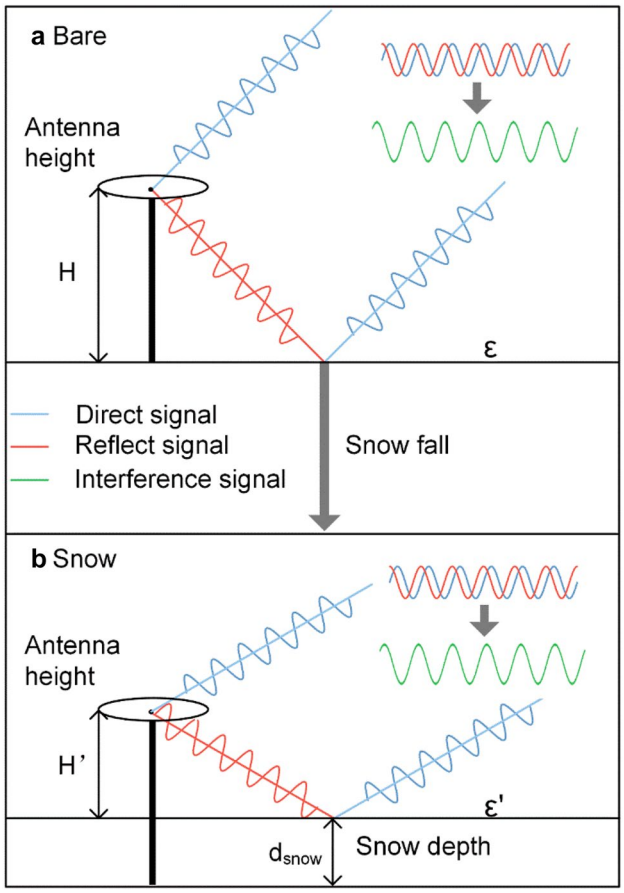

Fig. 1 Geometry model of GNSS antenna height and multipath signals propagation. H and H' denote the antenna height from reflection surface covered with and without snow, respectively, and the snow depth is denoted as the difference between H and H'. (Credit: Larson and Small 2014; Yu et al. 2015)

$$d = H - H' \tag{2}$$

For GNSS, when considering only the effects of atmospheric delays, the carrier phase Φ_j (unit in meters) of a specific carrier wave j can be expressed as:

$$\Phi_j = \rho + c(t_r - t^s) + N_j \times \lambda_j + T + M_j - I_j + \varepsilon_j \tag{3}$$

where ρ denotes the geometrical distance between receiver and satellite, c stands for the speed of light, t_r and t^s are the receiver clock bias and satellite clock bias, respectively. N_j is the integer ambiguity, λ_j is the specific carrier wavelength (unit in meters), T and I_j refer to tropospheric and ionospheric delays and ε_j is the sum of unmodeled errors. M_j is the carrier phase errors induced by multipath (unit in meters):

$$M_j = \frac{\lambda_j}{2\pi} \cdot \left(\tan^{-1} \frac{\alpha \sin \delta\phi}{1 + \alpha \cos \delta\phi} \right) \tag{4}$$

where the amplitude attenuation factor, α, reads as:

$$\alpha = \frac{A_r}{A_d} \tag{5}$$

where A_r and A_d denote to the amplitudes of the reflected and direct signals, respectively. The amplitude attenuation factor depends on the reflectivity of the reflector and is also influenced by the antenna gain pattern. Assuming $A_r \ll A_d$, the equality in (4) can be simplified to:

$$M_j = \frac{\lambda_j}{2\pi} \cdot \left(\tan^{-1}(\alpha \sin \delta\phi) \right) \tag{6}$$

Since $\alpha \sin \delta\phi \ll 1$, M_j can be further approximated to the damped sinusoid (Yu et al. 2015; Nievinski and Larson 2014a):

$$M_j = \frac{\lambda_j}{2\pi} \cdot (\alpha \sin \delta\phi) = \frac{\lambda_j}{2\pi} \cdot \left(\alpha \sin(2\pi \frac{2H}{\lambda_j} \sin \varepsilon) \right) \tag{7}$$

when taking $\sin \varepsilon$ as an independent variable, M_j can be expressed as:

$$\begin{cases} M_j = \frac{\lambda_j}{2\pi} \cdot \alpha \sin(2\pi \times \omega \times x) \\ \omega = \frac{2H}{\lambda_j} \\ x = \sin \varepsilon \end{cases} \tag{8}$$

The antenna height is linear with the frequency of carrier phase errors. Therefore, the antenna height can also be derived from a linear combination of carrier phase errors.

Triple-frequency combination is a generalization of the dual-frequency combination L4, which is free of geometric parameters and widely used in cycle slips detection and ionospheric monitoring (Simsky 2006). Moreover, the first-order ionospheric delays can also be removed by a simple linear combination of triple-frequency carrier phases (Montenbruck et al. 2010; Hauschild 2017):

$$\begin{aligned} M_{1,2,3} &= \kappa_1 \cdot \Phi_1 + \kappa_2 \cdot \Phi_2 + \kappa_3 \cdot \Phi_3 \\ &= \kappa_1 \cdot M_1 + \kappa_2 \cdot M_2 + \kappa_3 \cdot M_3 + u \end{aligned} \tag{9a}$$

$$u = \kappa_1 \cdot \lambda_1 \cdot N_1 + \kappa_2 \cdot \lambda_2 \cdot N_2 + \kappa_3 \cdot \lambda_3 \cdot N_3 \tag{9b}$$

where κ_1, κ_2 and κ_3 denote the coefficients of the linear combination, u is a constant unless there are cycle slips. Arbitrary coefficients that satisfy conditions $\kappa_1 + \kappa_2 + \kappa_3 = 0$ and $\kappa_1 \cdot \lambda_1^2 + \kappa_2 \cdot \lambda_2^2 + \kappa_3 \cdot \lambda_3^2 = 0$ can be used to form geometry- and ionospheric-free functions. To uniquely determine the coefficients, we impose additional normalizing conditions:

$\kappa_1 > 0$ and $\kappa_1^2 + \kappa_2^2 + \kappa_3^2 = 1$. Finally, the coefficients can be expressed as:

$$\begin{cases} \kappa_1 = \dfrac{\lambda_3^2 - \lambda_2^2}{\Lambda} \\ \kappa_2 = \dfrac{\lambda_1^2 - \lambda_3^2}{\Lambda} \\ \kappa_3 = \dfrac{\lambda_2^2 - \lambda_1^2}{\Lambda} \end{cases} \tag{10a}$$

$$\Lambda^2 = (\lambda_3^2 - \lambda_2^2)^2 + (\lambda_1^2 - \lambda_3^2)^2 + (\lambda_2^2 - \lambda_1^2)^2 \tag{10b}$$

Actually, the triple-frequency combination (9a) is equivalent to a combination of the three multipath errors for each respective carrier and thus is related to antenna height.

Since the frequency of the periodic oscillation of the multipath combination is proportional to antenna height, normally the snow depth can be retrieved by modeling it as a linear function of the spectral peak frequency of the triple-frequency phase combination:

$$H = a \times f + b \tag{11}$$

where a and b are the linear fitting parameters, H is the vertical distance from antenna to reflection surface, f stands for the peak frequency of the combined phase time series, which can be obtained by exploiting Lomb–Scargle spectral analysis (Press and Rybicki 1989).

Problems of the traditional triple-frequency method

Due to the different orbital parameters (CSNO 2017; EU 2016; GPS Directorate 2013), the revisit periods of BDS MEO and Galileo satellites are much longer than that of GPS (Table 1 and Fig. 2), and the distributions of the reflected signals are more scattered (Fig. 2). Therefore, the peak frequencies of BDS and Galileo phase combinations are more susceptible to the terrain variation around the GNSS antenna. The terrain variation refers to the difference of antenna height among multiple tracks located at different azimuths in the field. As shown in Fig. 3, for BDS and Galileo, despite the lack of sidereal repeatability, the satellite azimuth in BDS and Galileo occurs at a finite number of discrete lines. Therefore, the azimuth clustering can also be applied in BDS and Galileo and expanded to the Multi-GNSS triple-frequency method.

Table 1 Revisit periods of GPS, Galileo and BDS constellations (Pan et al. 2017)

Item	Revisit period (days)
GPS	1
Galileo (except FOC-1 and FOC-2 satellites)	10
Galileo (FOC-1 and FOC-2 satellites)	20
BDS (GEO and IGSO satellites)	1
BDS (MEO satellites)	7

Supposing the antenna height is H when the surface is snow free and H' in case the surface is covered with snow, the snow depth d_{snow} can be retrieved from the variations of antenna height. Since GPS ground tracks have sidereal repeatability, each satellite will reappear at four fixed azimuths as shown in the top of Fig. 3. Meanwhile, the bare ground height remains constant over time in GPS, and thus, the effects of terrain variation can be fully removed:

$$H' = \frac{1}{4}\sum_{i=1}^{4}(H_i + \Delta h_i + e_i) \tag{12}$$

where H_i denotes the antenna height of the i-th track, assuming the bare ground trend in the range is unchanged, it is a constant, and e_i is the error for each individual height retrieval.

The antenna height H during the snow-free period and the snow depth d_{snow} can be expressed as:

$$H = \frac{1}{4}\sum_{i=1}^{4}H_i \tag{13}$$

$$d_{\text{snow}} = H - H' = -\frac{1}{4}\sum_{i=1}^{4}(\Delta h_i + e_i) \tag{14}$$

However, for BDS and Galileo, the effects of terrain variation will not be mitigated in this simple way and will lead to an additional error, E_{terrain}, in snow depth estimation:

$$H' = \frac{1}{m}\sum_{i=1}^{m}(H_i + \Delta h_i + e_i) \tag{15}$$

$$H = \frac{1}{n}\sum_{i=1}^{n}H_i \tag{16}$$

$$d_{\text{snow}} = H - H' = -\frac{1}{m}\sum_{i=1}^{m}(\Delta h_i + e_i) + E_{\text{terrain}} \tag{17}$$

$$E_{\text{terrain}} = \frac{(m-n)\sum_{i=1}^{m}H_i + m\sum_{i=m+1}^{n}H_i}{m \times n} \quad (m < n) \tag{18}$$

where the index m denotes the number of azimuth clusters for a single day, n is the total number of the azimuth clusters.

In addition, we should be aware that there are 10 different triple-frequency phase combinations among five frequencies of Galileo signals: E1, E5a, E5b, E5 (E5a + E5b) and

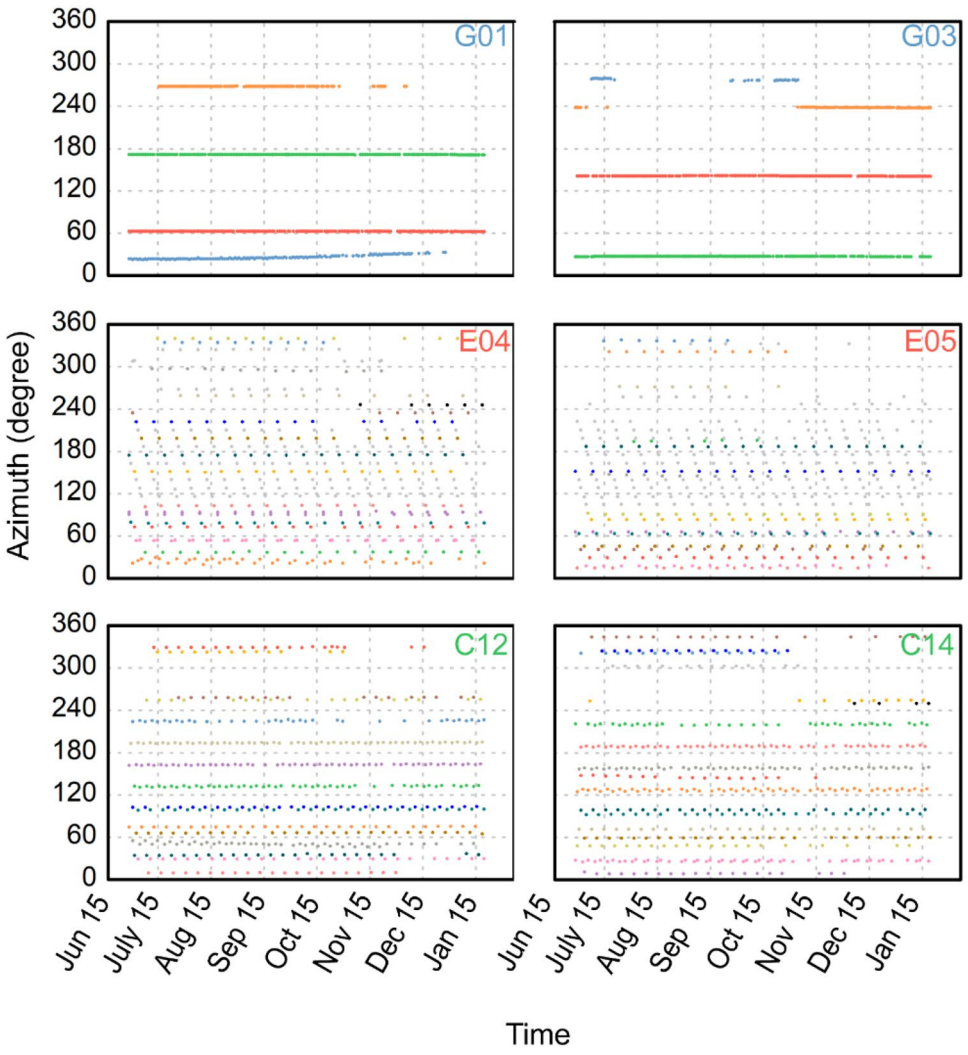

Fig. 2 Clusters of GPS (top), Galileo (middle) and BDS (bottom) satellite tracks at station SG27 during the observation period (June 15, 2018, to January 15, 2019). The clustering is based on the azimuth of satellite tracks. The different colors refer to the different clusters of the observation. The identifier on the upper right corner of each subgraph represents the satellite system and satellite number

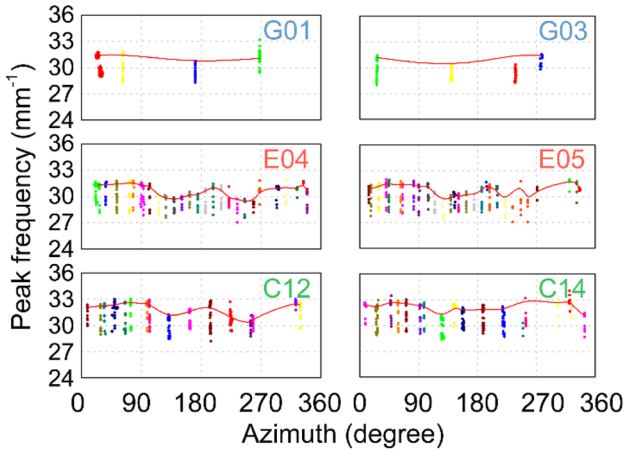

Fig. 3 Distributions of the peak frequencies of GPS (top), Galileo (middle) and BDS (bottom) phase combinations. The red line is the effects of terrain variations surrounding the GNSS antenna

E6. Therefore, it is necessary to evaluate the performance of various Galileo triple-frequency combinations and select the appropriate ones to estimate the snow depth.

Improved method

In this section, we propose an improved approach, which is applicable to not only GPS but also BDS and Galileo. The proposed method can effectively remove terrain effects. In addition, as discussed above, since there are 10 different triple-frequency combinations for Galileo satellites, the choice of linear combinations among multi-frequency needs to be discussed.

Procedures of the improved approach

The terrain effects on GPS-R have been investigated in several studies. Zhang et al. (2017) proposed a method to retrieve accurate snow depth observations of the horizontal

reflecting zone in the grid model, which needs a digital elevation model (DEM). Focusing on the SNR method of GPS and GLONASS, Tabibi et al. (2017) corrected the terrain effects by fixing the vertical datum. In this study, we propose an approach to compensate for the terrain variation by azimuth clustering without the need for a DEM, which is more suitable for multi-GNSS triple-frequency snow depth retrieval.

Figure 4 shows the flowchart of the improved approach in detail. Compared with the traditional method, to compensate terrain variation errors of BDS and Galileo, the clustering algorithm and normalization method are introduced in the data processing. The observables of multipath phase combinations can be clustered based on their azimuths. The peak frequencies can be obtained by exploiting Lomb–Scargle spectral analysis. For each cluster, the peak frequency of bare ground can be calculated from the average of the snow-free periods. The normalized peak frequency of each cluster can be obtained by removing the peak frequency of the bare ground. Azimuth clustering, based on repeatability of the GNSS tracks, offers an effective strategy for comparing similar azimuths.

In order to extract the terrain effects surrounding the antenna, the mean peak frequency of each azimuth cluster under snow-free conditions is calculated separately. As shown in Fig. 5, after the mean peak frequency of each cluster was removed, most of the observations are converted to a range below 0. The blue line shown in the figure reflects the maximum snow depth in each azimuth cluster, which is affected by the characteristics of the scattering surface and the revisit time of the satellite. In contrast, the red line in Fig. 3 refers to the effects of terrain variations surrounding the GNSS antenna,

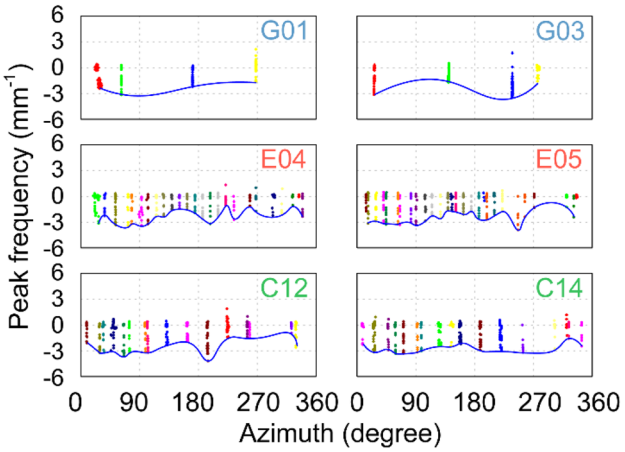

Fig. 5 Distributions of the peak frequencies derived from BDS and Galileo phase combinations with terrain variation errors removed

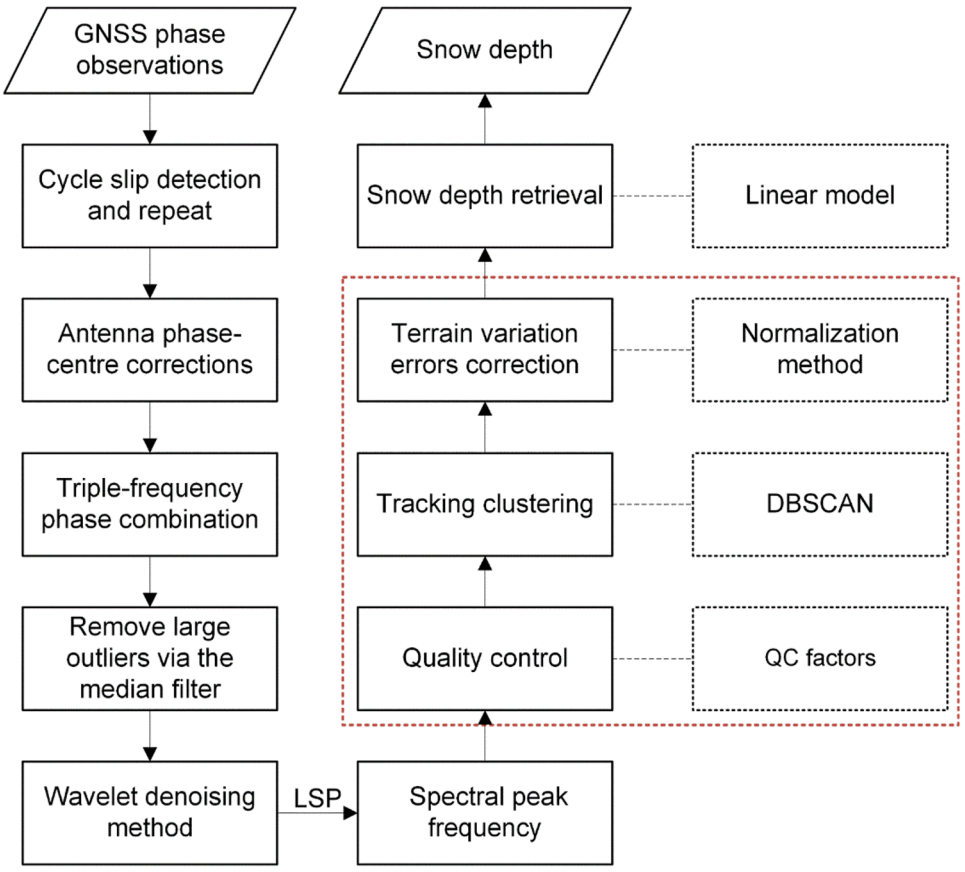

Fig. 4 Procedures of the improved approach. The main difference between the improved method and the traditional one is shown in the red dashed box

which can be obtained from the average of peak frequencies during the snow-free period. As described above, the peak frequency will reduce for increased accumulated snow and vice versa, which means the snow depth is derived from the variation of peak frequency rather than the absolute value of frequency. Therefore, peak frequency normalization preprocessing will not influence the snow depth estimated from peak frequency and will be free from topographic variation.

For each cluster, the snow depth d_i can be expressed as:

$$\begin{cases} d_i = H_{i,\text{bare}} - H_{i,\text{snow}} = k_i \times f_{i,\text{nor}} \\ H_{i,\text{bare}} = a \times \widehat{f_{i,\text{bare}}} + b \\ H_{i,\text{snow}} = a \times f_{i,\text{snow}} + b \\ f_{i,\text{nor}} = \widehat{f_{i,\text{bare}}} - f_{i,\text{snow}} \\ k_i = -a \end{cases} \tag{19}$$

where $f_{i,\text{nor}}$ stands for the normalized peak frequency of triple-frequency phase combination, $\widehat{f_{i,\text{bare}}}$ is the average of the peak frequency of combination during the snow-free period, $f_{i,\text{snow}}$ refers to the unnormalized peak frequency. k_i is the fitting coefficient, which can be calculated from the historical or simulated antenna height and spectral peak frequency by linear fitting. Figure 6 shows the relationship between the simulated snow depth and spectral peak frequency; the fitting coefficients are summarized in Table 2. The averaged snow depth estimation, d_{snow}, is given by:

$$d_{\text{snow}} = \frac{1}{n}\sum_{i=1}^{n} d_i \tag{20}$$

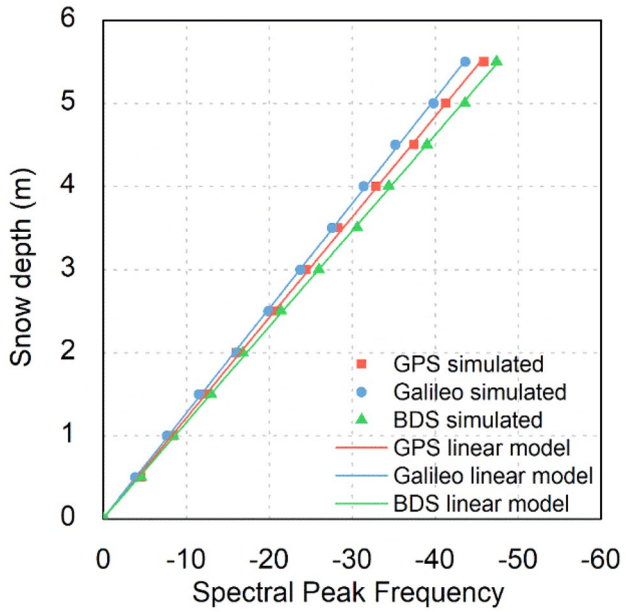

Fig. 6 Relationship between the simulated snow depth and spectral peak frequency. The simulation parameters are given in Table 3

Table 2 Fitting coefficients obtained from the simulated observations. L1, L2 and L3 refer to the wavelength of each carrier (units in meter)

System	Combination	k	L1 (m)	L2 (m)	L3 (m)
GPS	L1 + L2 + L5	−0.1218	0.1903	0.2442	0.2548
Galileo	E1 + E5a + E5b	−0.1268	0.1903	0.2548	0.2483
	E1 + E5a + E6	−0.1160	0.1903	0.2548	0.2344
BDS	B1 + B2 + B3	−0.1171	0.1920	0.2483	0.2363

Since the characteristics of the scattering surface within a limited area are similar, the adjacent clusters can be merged into a new cluster. For a specific navigation system, these preliminary spare clusters within an azimuth angle of 30 degrees are further binned together, regardless of the satellite identification number. The preliminary sparse clusters refer to the clusters of BDS and Galileo shown in Figs. 3 and 5. However, it is not necessary to do so for GPS because of plenty of observations on each cluster. With a multistep clustering processing, the snow depth can be retrieved from each cluster continually. Since the snow depth is estimated from the normalized peak frequency, the improved method can eliminate most of the errors caused by terrain variations.

Theoretical performance of different phase combinations

Assuming each carrier phase has the same measurement noise (e.g., $\sigma_0 = \sigma_1 = \sigma_2 = \sigma_3 = 1$ cm), the normalizing condition $\kappa_1^2 + \kappa_2^2 + \kappa_3^2 = 1$ ensures that the noise of the triple-frequency combination will match that of the individual carrier phases (i.e., $\sigma_M = 1$ cm; Montenbruck et al. 2010; Hauschild 2017). For comparison of different linear combinations, we evaluate the snow depth retrieval performance of all possible triple-frequency phase combinations of Galileo by simulation tests. The simulation parameters are summarized in Table 3 (Nievinski and Larson 2014b).

Figure 7 shows an example of the combined phase error pattern with respect to $\sin\theta$ and their power spectral density (PSD). Table 4 summarizes the coefficients of the linear combination, the maximum absolute carrier phase multipath

Table 3 Parameters of the combined phase error simulations

Item	Parameters
Antenna gain pattern	TRM59800.80
antenna height	2.5 m
Elevation angle	5°–25°
Signals	E1/E5/E5a/E5b/E6
Surface materials	Snow
Noise	Set as white noise (1 cm SD)

errors, and the corresponding PSD of the 10 triple-frequency combinations possible for the five Galileo carriers. Since the random noise of each combination is of the same magnitude, the maximum of PSD is equivalent to the peak/noise ratio. As can be observed from Fig. 7 and Table 4, the phase multipath errors and corresponding PSD are different among the 10 combinations; the corresponding PSD of some phase combinations is significantly weaker than that of others. From the perspective of peak/noise ratio, the worst combination is E5b + E5a + E5, and the best combination is E1 + E5a + E6. It is worth mentioning that the carrier phase multipath errors, as well as the corresponding PSD, will change in scale and the scale factor will be different for a specific combination with different normalizing conditions (κ_1, κ_2 and κ_3) or measurement noises (σ_M). However, the peak frequency of the spectrum of the multipath phase sequence will not be changed.

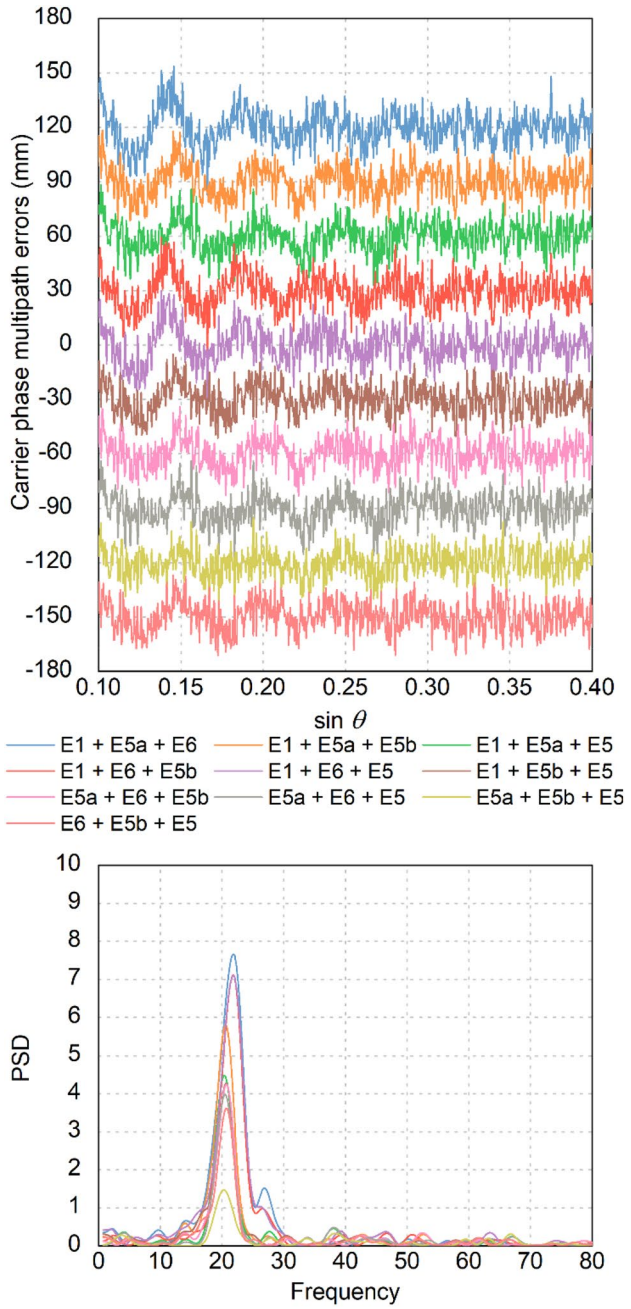

Fig. 7 Carrier phase multipath errors (top) and PSD (bottom) of all possible triple-frequency combinations for Galileo. The carrier phase multipath errors were extracted from the linear combination (9a), and they were evenly shifted in the vertical to be clearly shown. The PSD can be obtained by exploiting Lomb–Scargle spectral analysis

Data set and processing

The EarthScope Plate Boundary Observatory (PBO) GNSS network uses geodetic GNSS receivers and antennas to measure and monitor earth deformation. The observation data used in our study were collected at the station SG27 (71.32° N and 156.61° W) of the PBO network in Alaska (Fig. 8), tracking the four GNSS (GPS/GLONASS/Galileo/BDS) constellations (http://www.unavco.org/), and the in situ reference values of snow depth were collected by the co-located climate station PABR, which can be obtained from the National Operational Hydrologic Remote Sensing Center (http://www.nohrsc.noaa.gov/). The climate station is 7.2 km away from the GNSS station. Since the region is a vast and flat tundra stretching hundreds of kilometers, rather than a mountainous region, the snow depth observation of the climate station can be regarded as the reference values of the GNSS-R results. The GNSS station is equipped with a SEPT POLARx5 receiver, and the antenna TRM59800.80 is covered with a SCIS radome. The triple-frequency signals of GPS/BDS/Galileo can be tracked continuously at an interval of 15 s. In order to estimate snow depth, GNSS observables from June 15, 2018 (summer), to January 15, 2019 (winter), were used. As shown in Fig. 8, there was an open area around the antenna (http://earth.google.com/ and http://www.unavco.org/). The DEM around the station SG27 is also shown in Fig. 8 (http://www.usgs.gov/).

In the process of triple-frequency phase snow depth retrieval, all the GPS and BDS phase observations are applied. Galileo phase combinations with a high peak/noise ratio were also used to evaluate the performance of different phase combinations, respectively. The PSD noise is calculated based on the average of PSD in the noise range between 0 and 40 mm^{-1}. The elevation mask was set to 5°, and the maximum satellite elevation angle of the signal was set to 30°. Moreover, to offset the terrain variation errors, the clustering algorithm and the normalization method were employed. The processing strategies of triple-frequency snow depth retrieval can be found in Table 5.

Unpredictable events, such as thermal additive noise and multiplicative noise in the phase measurements or the

Table 4 Coefficients of the linear combination, maximum absolute carrier phase multipath errors and the corresponding PSD of the 10 triple-frequency combinations possible of the five Galileo carriers

Combination	κ_1	κ_2	κ_3	Maximum of PSD	Maximum absolute phase multipath errors (mm)
E1 + E5a + E6	0.2792	0.5249	− 0.8041	7.78	53.91
E1 + E5a + E5b	0.0846	0.6610	− 0.7456	5.99	34.56
E1 + E5a + E5	0.0421	0.6851	− 0.7272	4.59	33.81
E1 + E6 + E5b	0.2077	− 0.7877	0.5800	7.27	51.13
E1 + E6 + E5	0.2448	− 0.7970	0.5522	7.23	46.33
E1 + E5b + E5	0.0430	− 0.7276	0.6846	4.46	34.26
E5a + E6 + E5b	0.5390	0.2617	− 0.8006	4.43	33.03
E5a + E6 + E5	0.6351	0.1269	− 0.7620	4.02	35.75
E5a + E5b + E5	0.4003	0.4161	− 0.8164	1.53	36.42
E6 + E5b + E5	0.1479	− 0.7694	0.6214	3.80	35.22

E1: 19.0 cm; E6: 23.4 cm; E5b: 24.8 cm; E5: 25.2 cm; E5a: 25.5 cm

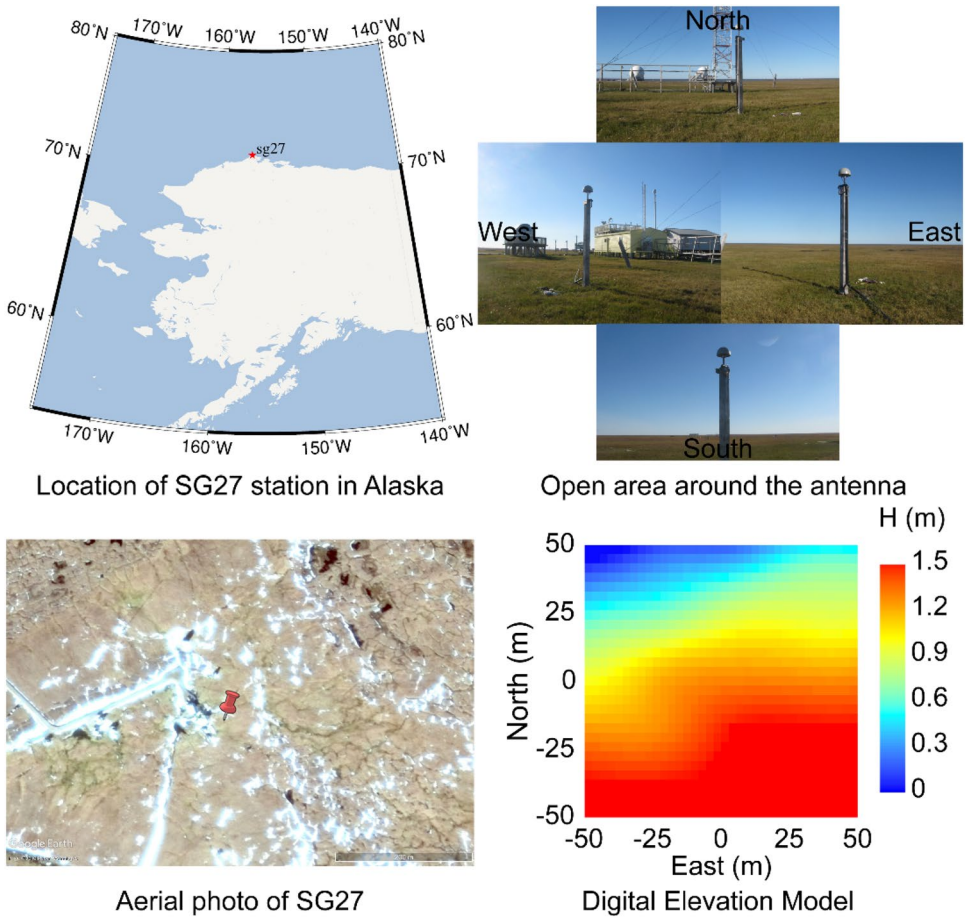

Fig. 8 Geographical location of the GNSS observatory station. The SG27 site is in an open area, equipped with a SEPT POLARx5 receiver and TRM59800.80 antenna. An aerial photograph is also shown in the lower-left corner of this figure. The DEM obtained from United States Geological Survey (USGS) is used for the description of the terrain variation surrounding the antenna

degradation on observables induced by ionospheric scintillation, result in unmodeled errors. As shown in Fig. 9, the signals will be contaminated by the unmodeled errors, and the spectral peak frequency of the multipath phase series will deviate from the true values obviously. When the combined phase observations are contaminated by overlapped peaks, it is difficult to distinguish the main peak and the secondary peak in the spectrum. In addition, the main peak will be overwhelmed when the combined phases are contaminated by large noise (middle row panels). In order to detect and eliminate such outliers, the snow depth retrieval procedure must be complemented with effective quality

Table 5 Processing strategies of triple-frequency snow depth retrieval

Item	Processing strategies
Observation	Triple-frequency multipath combination (Simsky 2006)
Signal selection	G: L1 + L2 + L5
	C: B1 + B2 + B3
	E (with high peak/noise ratio): E1 + E5a + E5b and E1 + E5 + E6
	E (with low peak/noise ratio): E5a + E6 + E5b and E5a + E6 + E5
Sampling rate	15 s
Elevation angle	5°–30°
Satellite orbit	Precise orbit products from IGS analysis centers
Coordinate of the station	Fixed using SINEX product
Terrain variation errors	Corrected
Clustering algorithm	Density-based spatial clustering of applications with noise (DBSCAN) (Ester et al. 1996); angular tolerance of 2.5°; minimum number of points per cluster of 10

control techniques. In general, the minimum elevation span of the satellite tracks was set to 10°, and the duration of each measurement was no longer than 1.5 h. Inspired by Wang et al. (2018), who used the wavelet decomposition to retrieve the sea level based on SNR observation, we used a similar method for phase combinations denoising (Torrence and Compo 1998; Wang et al. 2018). Moreover, to detect and remove those signals which were corrupted by unmodeled noise, the peak/noise ratio and the ratio of the central peak with side peak were also used as the quality control targets. It is worth mentioning that the quality control in snow-free conditions is more stringent for the lower noise of the signals reflected from the bare ground. In this regard, the quality control index of each navigation system should set up separately. These empirical quality control parameters derived from historical data are applicable to most GNSS stations. However, one should be aware that the most appropriate parameters will be slightly different for different stations. Such a difference is marginal for snow depth monitoring (Table 6).

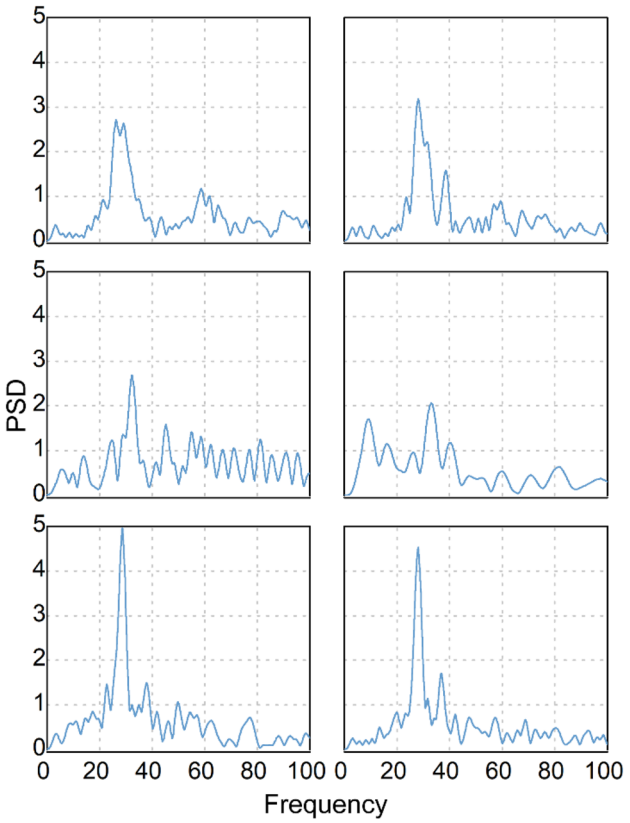

Fig. 9 Spectrogram of anomalies of triple-frequency phase combination. Top: observations contaminated by overlapped peaks. Middle: observations contaminated by large noise. Bottom: normal observations. The cases were obtained from different satellites with the same linear combination on the same day

Results and discussion

The improved method has extended the GPS triple-frequency snow depth retrieval to another GNSS system by correcting the terrain variations error. The first experiment shows the comparisons of the snow depth estimates using the traditional and proposed methods, respectively. In the second experiment, we evaluated the performance of triple-frequency combinations with high and low peak/noise ratio on snow depth estimation, respectively. Additionally, the precision of the triple-frequency snow depth estimated with different navigation systems was compared. Finally, we evaluate the performance of the proposed approach when applied to the SNR and L4 method.

Table 6 Quality control indexes of triple-frequency snow depth retrieval

Item	Processing strategies
Difference of max and min elevation angle	> 10°
The duration of measurements	< 1.5 h
Peak/noise ratio	Snow free: G: > 14.5 C: > 12.5 E: > 13.5
	Snow: G: > 10.5 C: > 8.5 E: > 9
The ratio of the central peak and side peak	Snow free: G: > 2.5 C: > 2 E: > 2
Filter	Wavelet method

G, C and E, respectively, refer to GPS, BDS and Galileo

Validation of the improved method

In order to evaluate the performance of the improved triple-frequency retrieval method, first, the snow depth time series were estimated. Second, the peak frequency observation was processed by the DBSCAN algorithm and normalization method to avoid being influenced by the errors due to the topography. Third, we processed the phase data using the traditional method presented by Yu et al. (2015) as a contrast. The snow depth is the average snow depth estimate derived from phase combinations from all valid GNSS tracks. As shown in Fig. 10, during the experiment, the snow depth estimations using the improved triple-frequency method with the BDS (B1 + B2 + B3) or Galileo (E1 + E5a + E5b) observations are much closer to the in situ measurements, while the snow depth estimated by the traditional technique presents a larger fluctuation. Hence, the poor performance of the traditional method can be attributed to the influence of terrain variation errors.

It is noticed that the snow depth residuals under snow conditions are obviously larger than those under snow-free conditions. This can be attributed to signal penetration. More specifically, the GNSS signals partly reflected at snow surface as a specular reflector, while some components of waves reflected under the snow surface and reached the antenna with a slightly longer excess propagation path (Ozeki and Heki 2012). In addition, since the snow depths are averaged over all azimuth clusters surrounding the antenna, the larger uncertainty might be a result of the spatial heterogeneity in snow cover over multiple tracks. Compared to the soil surface, the spatial heterogeneity is significantly greater for the snow-covered surface (Gutmann et al. 2012).

As illustrated in the black dashed boxes in Fig. 10, the residuals increase remarkably when the snow depth varies sharply in a short time. This is probably because the reflection surface characteristics such as roughness and surface slope changed significantly with the sharp variations in cumulative precipitations. Moreover, the reference snow depths were recorded from the co-located climate station twice a day, while the snow depth estimates were the average of dozens of observations throughout the day. The in situ snow depth records are definitely more accurate due to the sparse samplings, but some details of the snow depth variations may be missed. For example, snowfall happens to occur between two snow depth records.

Furthermore, the snow depth estimations from the traditional method illustrate a more evident deviation than those from the improved method. Figure 11 shows the residual distributions of snow depth estimates derived from the traditional and proposed methods for BDS and Galileo. As shown in Table 7, the mean residual values decrease from − 1.1 cm for Galileo and − 1.5 cm for BDS to near zero, while the RMSEs decrease from 4.3 and 5.6 cm to 2.6 and 3.5 cm, respectively, once the proposed method was applied.

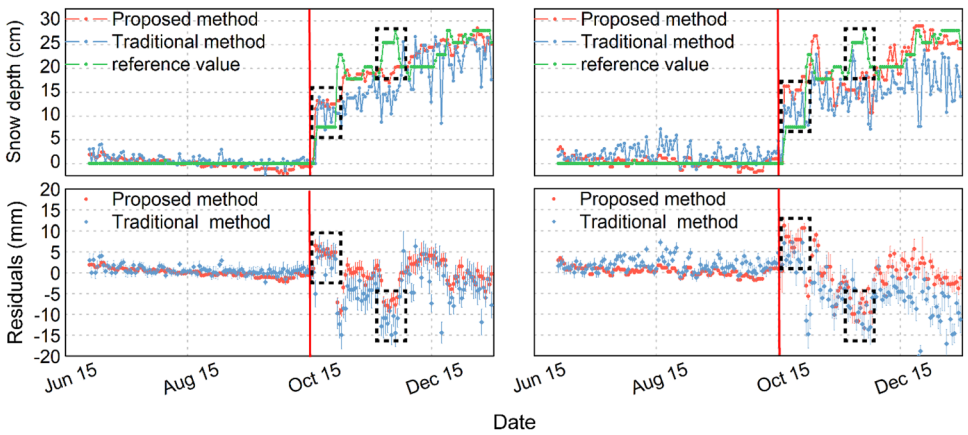

Fig. 10 Comparisons of the snow depth estimates and errors between the traditional and proposed method (left: Galileo E1 + E5a + E5b; right: BDS B1 + B2 + B3). Vertical error bars in the lower panels denote the standard error of snow depth. Some of the large residuals are shown in black dashed boxes. Results are divided into snow free and snow periods by vertical red lines

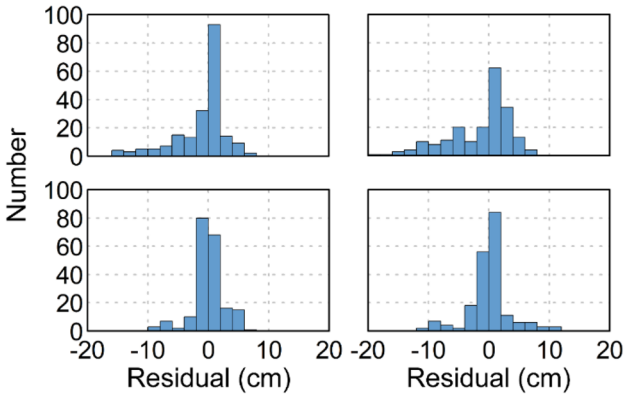

Fig. 11 Residual distributions of Galileo (left) and BDS (right) snow depth estimation derived from the traditional (top) and proposed (bottom) method, respectively

Table 7 Mean, RMSE and correlation coefficient in BDS, Galileo and GPS snow depth estimation

System	Method	Mean (cm)	RMSE (cm)	Correlation coefficient
Galileo	Traditional	−1.1	4.3	0.93
	Proposed	0	2.6	0.97
BDS	Traditional	−1.5	5.6	0.91
	Proposed	0.1	3.5	0.95
GPS	Traditional	−0.3	2.6	0.98
	Proposed	−0.2	2.5	0.98

The correlation coefficients of the proposed and traditional method are, respectively, 0.97 and 0.93 for Galileo, 0.95 and 0.91 for BDS. Therefore, the proposed method shows better performance than the traditional method in terms of accuracy and precision. Compared with the remarkable improvement for BDS and Galileo, the performance of the proposed method and the traditional one shows similar results for GPS. This is reasonable since the sidereal (azimuth) repeatability of ground tracks in GPS makes the terrain correction less necessary.

Experimental performance of different phase combinations

Galileo phase combinations with high and low peak/noise ratio (E1 + E5a + E5b and E1 + E5 + E6) and (E5a + E6 + E5b and E5a + E6 + E5), respectively, were used to analyze the performance of various combinations. As shown in Fig. 12, the multipath phase combinations with low peak/noise ratios were corrupted by unmodeled noise, resulting in overlapped peaks and peak frequency shifts to the lower or higher frequencies. In most cases, there is no dominant peak in the frequency domain. As investigated by Montenbruck et al. (2010) and Hauschild (2017), for a specific triple-frequency combination, the linear combination is dominated by signals which have proximate frequencies and similar weights, while the carrier phase multipath error of the other signal is strongly attenuated. For different combinations, the carrier phase multipath errors and corresponding PSD are determined by the wavelengths of each of the three carriers. The combinations consisting of three signals with similar frequency, such as E5a + E6 + E5b and E5a + E6 + E5, have a lower PSD at the main frequency and are not suitable for snow depth retrieval.

Figure 13 shows the daily averages of the snow depth estimates using E1 + E5a + E5b and E1 + E5 + E6 phase combinations with high peak/noise ratios. The estimations derived from these two combinations agree well with each other and show good agreements with the in situ snow depth observations. The correlation coefficients between

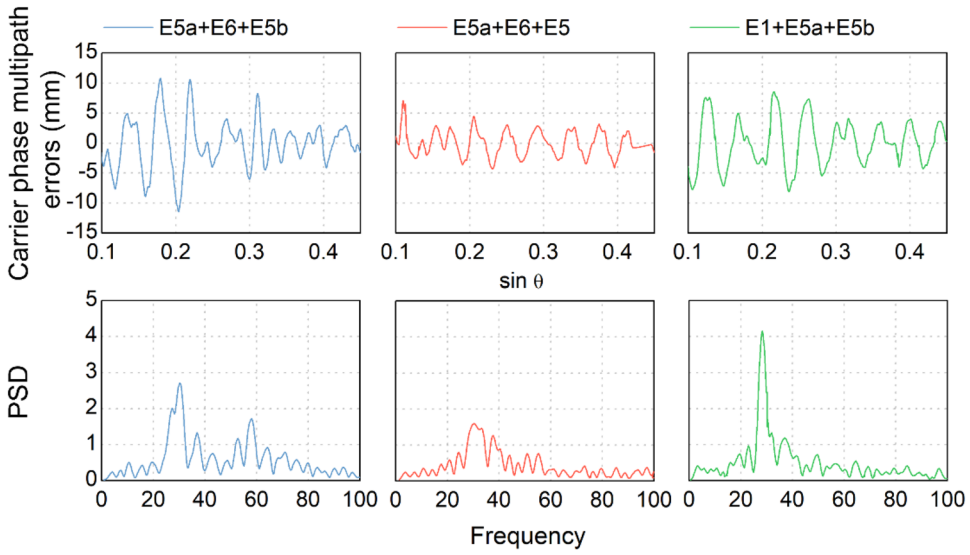

Fig. 12 Carrier phase multipath errors (top) and spectrograms (bottom) of the triple-frequency phase combinations with low peak/noise ratio (left and middle) and high peak/noise ratio (right)

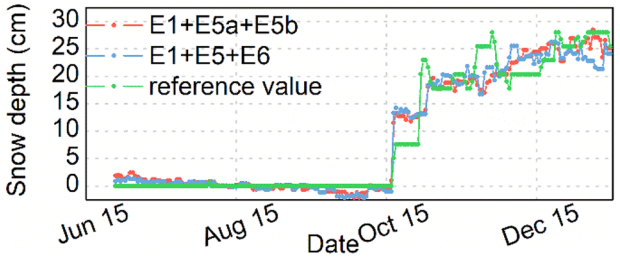

Fig. 13 Snow depth estimation obtained by using the combinations of Galileo E1 + E5a + E5b and E1 + E5 + E6 carrier phases, respectively

the snow estimations and in situ snow depth derived from E1 + E5a + E5b and E1 + E5 + E6 are 0.97 and 0.96, respectively.

Figure 14 shows the residuals of daily snow depth estimation derived from the combinations of Galileo E1 + E5a + E5b and E1 + E5 + E6 carrier phases. The histograms of snow depth estimation residuals are given in the figure as well. As shown in the left panel, the residuals are mainly distributed between -5 and 5 cm. The mean errors of snow depth estimation derived from E1 + E5a + E5b and E1 + E5 + E6 are 0 cm and 0.1 cm, and the corresponding RMSEs are 2.6 cm and 2.9 cm, respectively. Although the peak/noise ratio of E1 + E5a + E5b is slightly higher than that of the E1 + E5 + E6 phase combination, there is no statistically significant improvement in the results of snow depth retrieval. Similar results have been found in the snow depth estimation derived from other phase combinations with a high peak/noise ratio. According to the above analysis, Galileo signals can provide more opportunities to retrieve the snow depth well by using different triple-frequency phase combinations.

Performance of different navigation systems

In order to investigate the performance of different navigation systems, the triple-frequency phase combinations of L1 + L2 + L5 for GPS, E1 + E5a + E5b for Galileo, and B1 + B2 + B3 for BDS were used for validation. Figure 15 shows the time series of snow depth obtained from different constellations. The overall trends of snow depth estimated by each constellation are highly consistent with the in situ reference values. In terms of correlation, the correlation coefficient of the GPS phase combination is the largest, reaching 0.98, followed by Galileo with a correlation coefficient of 0.97, while the BDS correlation coefficient of 0.95 is the smallest.

Figure 16 shows the corresponding residuals as well as their statistics. In addition, the mean errors, RMSEs and correlation coefficients of the estimations derived from different navigation systems are shown in Table 8. Obviously, most of the residuals of Galileo and GPS are well within ± 5 cm, while those of BDS are slightly larger, with a variation of ± 10 cm. The main reason may be that the unmodeled error of the BDS phase observable is larger than that of GPS and Galileo phase measurements. However, even though the unmodeled error of Galileo phase measurement is approximately the same as that of GPS, the accuracy of snow depth estimated by Galileo phase combination is slightly worse than that of GPS, which has the highest accuracy, with an RMSE of 2.6 cm. It should be mentioned that, although the terrain variation errors can be mostly compensated by the proposed method, the effects of the topography change cannot be eliminated completely. The reference peak frequency used in the normalization is obtained by averaging during snow-free periods. However, the reflection region during the snow period is not exactly the same as that during the snow-free period. As the snow depth increases, the area of the reflection region decreases. Therefore, although most of the terrain errors can be removed by normalization, terrain errors caused by different reflection regions remain.

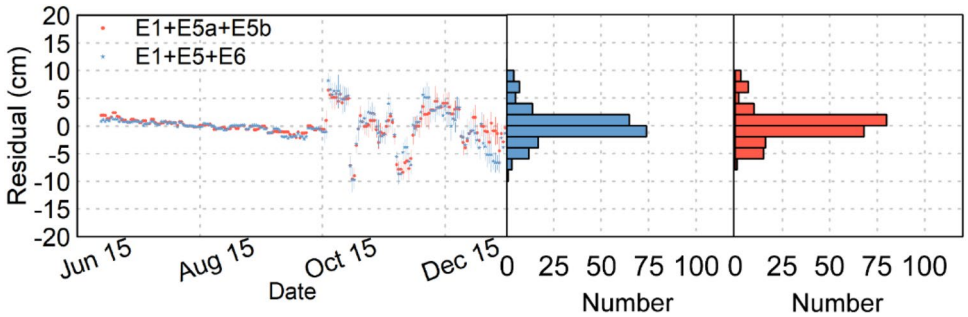

Fig. 14 Residuals between the snow depth estimations and in situ observables. Left: Residuals of daily snow depth estimation; vertical error bars denote the standard error of snow depth. Middle: Residual distributions of Galileo E1 + E5 + E6. Right: Residual distributions of Galileo E1 + E5a + E5b. The error bars represent the uncertainties of the snow depth estimation

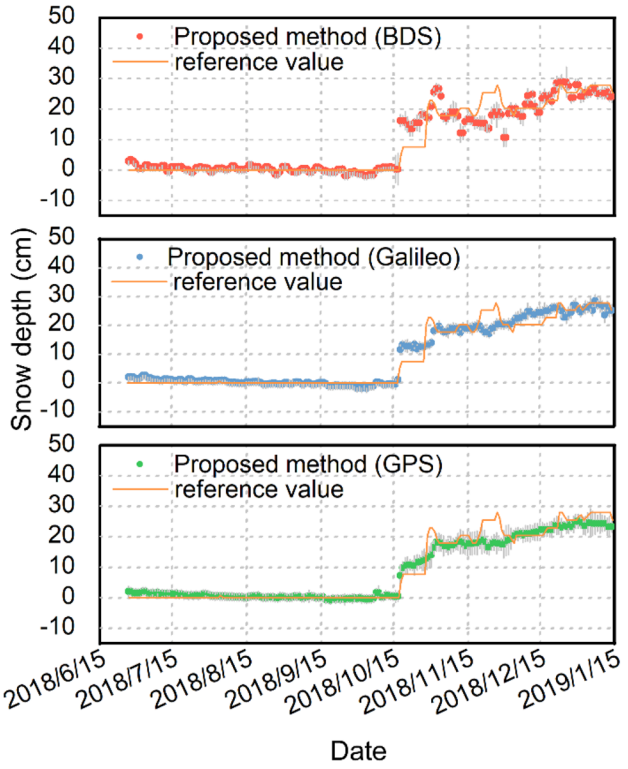

Fig. 15 Time series of snow depth estimation obtained from triple-frequency combinations. Gray vertical error bars denote the standard error of snow depth estimation

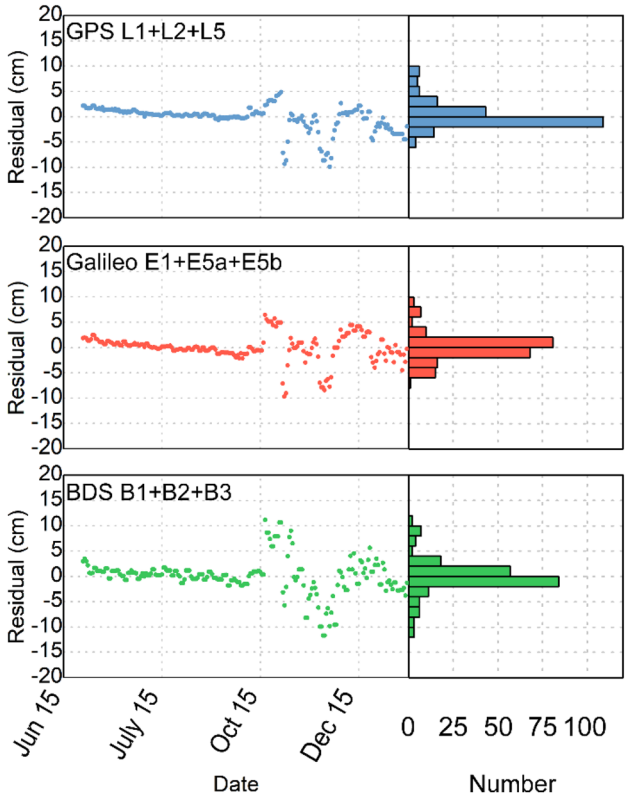

Fig. 16 Residuals between in situ observations and snow depth estimations. The snow depth estimation residuals obtained by using the combinations of GPS L1 + L2 + L5 (top), Galileo E1 + E5a + E5b (middle) and BDS B1 + B2 + B3 (bottom) carrier phases

Furthermore, since the snow depths derived from Galileo provide better azimuth coverage than the GPS estimation and the field snow depth measurements, such small differences between GPS and Galileo estimates are perfectly acceptable. It is also noticed that the residuals for all GNSS in snow-free conditions are smaller than those under snow conditions. As discussed above, the larger error during the snow period may be attributed to signal penetration and spatial heterogeneity in the snow surface, compared to the soil surface.

Application to SNR method and L4 method

The proposed approach can also be applied to the SNR and L4 (dual-frequency geometry-free linear combination, i.e., L1–L2) methods. Figure 17 shows the snow depth estimation derived from GPS L1 SNR observations. The results indicate that the estimation obtained from both the traditional method and the proposed one agrees well with the in situ snow depths. In terms of uncertainty, the proposed method showed an acceptable improvement, with STD decreases from 3.1 to 2.0 cm.

It should be mentioned that the SNR method is a single-frequency method; therefore, multiple independent snow depth retrievals are available for each GNSS in a multi-frequency receiver. To demonstrate the effectiveness of the proposed algorithm relative to the SNR method, we investigated the performance of all possible SNR derived snow depths both with and without terrain correction, and the results are summarized in Table 9. As shown in the table, all correlation coefficients of the estimates are improved simultaneously once the proposed terrain correction method has been applied. Meanwhile, the mean errors and STDs of the snow depth estimations are decreased to some extent after terrain correction.

Moreover, the proposed method can also be applied to the L4 method as well. Figure 18 shows the daily average of the snow depth estimated from GPS L4 (L2–L5) observations,

Table 8 Mean, RMSE and correlation coefficient in GPS/BDS/Galileo snow depth estimation

GNSS system	Mean (cm)	RMSE (cm)	Correlation coefficient
Galileo	0	2.6	0.97
BDS	−0.1	3.5	0.95
GPS	−0.3	2.5	0.98

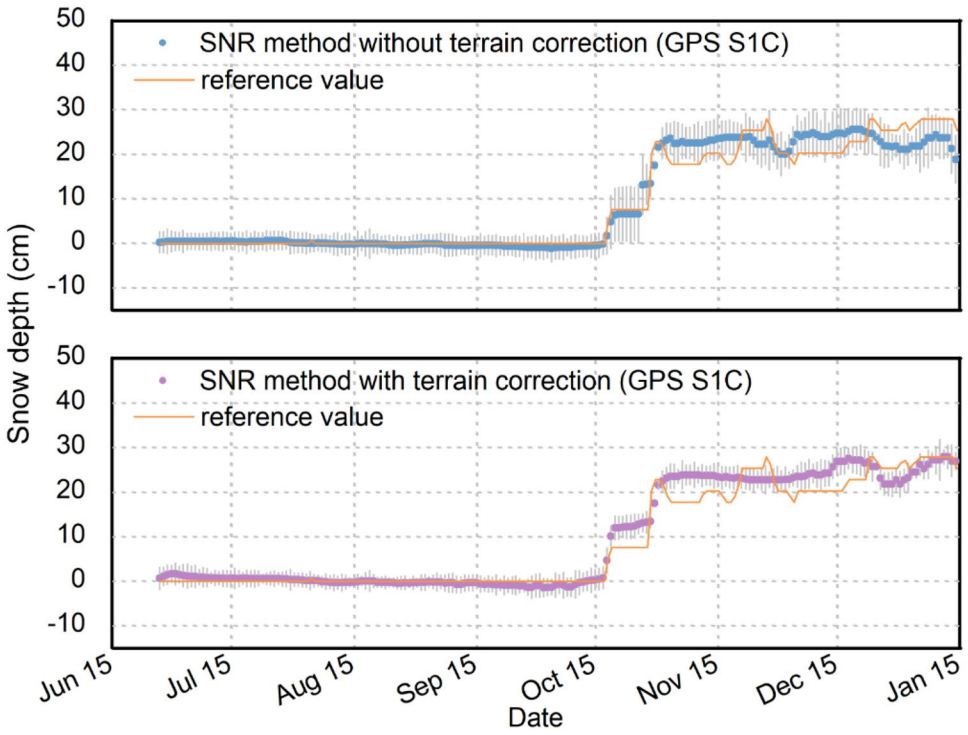

Fig. 17 Time series of snow depth estimation obtained from SNR combinations. Gray vertical error bars denote the standard error of snow depth estimation

Table 9 Mean, STD and correlation coefficient in BDS, Galileo and GPS snow depth estimated from SNR observations, both with (upper lines) and without (lower lines) the terrain correction

System	SNR observation	Mean (cm)	STD (cm)	Correlation coefficient
GPS	S1C	−0.7	2.0	0.98
		1.0	3.1	0.95
	S2L	−1	2.3	0.97
		−1.1	2.6	0.96
	S5Q	−1.3	1.5	0.96
		−2.0	1.8	0.95
Galileo	S1C	0	2.2	0.97
		−4.5	3.2	0.93
	S5Q	2.8	2.6	0.98
		3.0	2.6	0.93
	S8Q	3.8	2.5	0.96
		1.5	3.3	0.94
	S7Q	6.4	2.3	0.94
		2.7	2.7	0.89
	S6C	3.8	2.5	0.96
		−0.9	2.8	0.90
BDS	S2I	1.0	2.1	0.94
		4.7	3.0	0.90
	S7I	0.6	2.1	0.93
		−0.9	2.8	0.90
	S6I	1.7	2.2	0.94
		2.6	2.7	0.89

both with and without terrain correction. As shown in the figure and Table 10, the snow depth obtained from the proposed method shows a better agreement with the reference values and the correlation coefficient increases from 0.96 to 0.98.

Conclusions

An improved snow depth monitoring approach is proposed and evaluated using the triple-frequency phase combinations from different navigation systems. The main advantage of this method is that the topographic feature of the reflecting surface was considered for estimating the snow depth. Since the terrain variation error was corrected by using the DBSCAN algorithm and normalization method, the improved snow depth retrieval approach can be applied to other navigation systems, which have a greater azimuth coverage as well as longer revisit time. In terms of snow depth retrieval accuracy, the proposed method performed better than the traditional method by experiment for both BDS and Galileo.

For Galileo, the performance of snow depth retrieval is compared using the phase combinations with high and low peak/noise ratios, respectively. The triple-frequency phase combinations with low peak/noise ratios generally cannot be used for snow depth monitoring due to the overlapped peak and peak frequency shift in the frequency domain. The estimated snow depth obtained by using the phase combination

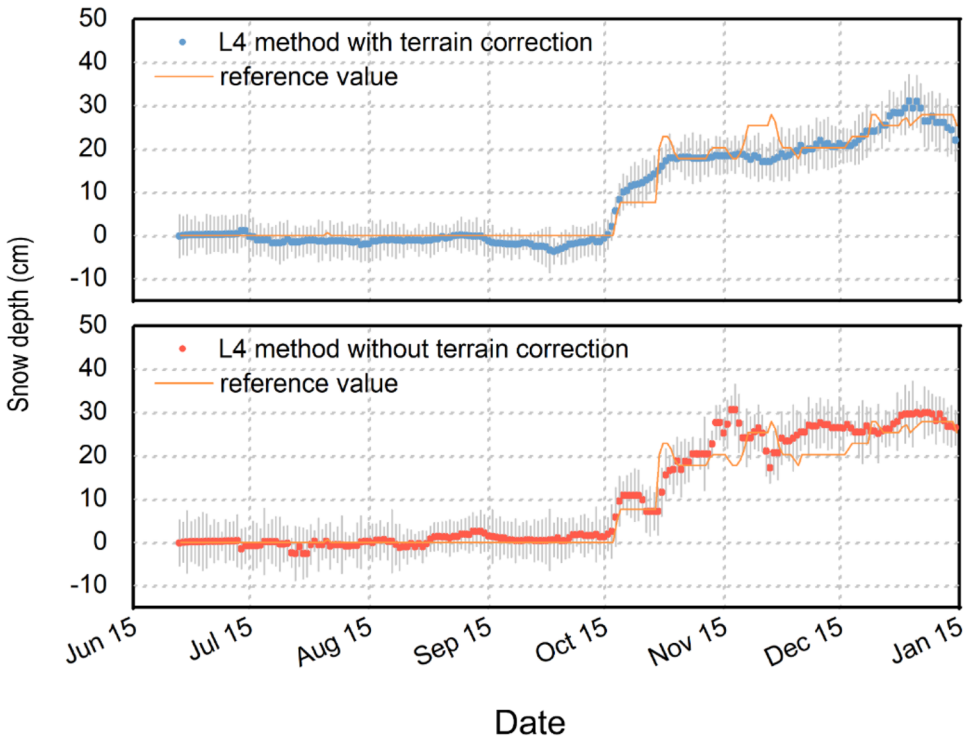

Fig. 18 Time series of snow depth estimation obtained from dual-frequency combinations. Gray vertical error bars denote the standard error of snow depth estimation

Table 10 Mean, STD and correlation coefficient in GPS snow depth estimated from L4 observations

Terrain correction	Mean (cm)	STD (cm)	Correlation coefficient
With	0.6	3.9	0.98
Without	− 1.4	4.5	0.96

with a high peak/noise ratio shows an excellent agreement with in situ snow depth measurement.

The results derived from phase combinations were compared with in situ snow depth observations from NOAA, showing a correlation coefficient of 0.98, 0.97 and 0.95 for GPS, Galileo, and BDS, respectively. The corresponding RMSEs are 2.5, 2.6 and 3.5 cm. Due to the relatively large unmodeled error of BDS phase observation, the snow estimation performance of the BDS phase combination method is slightly worse than GPS and Galileo, while the slight deviation between the GPS and Galileo estimation might be attributed to the different azimuth coverage. Moreover, it is demonstrated that the proposed approach can be extended to SNR and L4 methods.

The RINEX Working Group has announced the availability of RINEX 3.04 to support all publicly available signals as GNSS rapidly expands. Therefore, more optional phase combinations will be provided for snow depth monitoring. Future research will focus on the snow depth retrieval using multiple-frequency signals and multiple navigation constellations. Moreover, snow depth derived from different satellite navigation systems needs to be combined to improve the accuracy of the proposed method.

Acknowledgements We are grateful to the GNSS data provided by the Plate Boundary Observatory operated by UNAVCO (UNAVCO Community 2002) and the DEM data provided by USGS. We would also like to express our gratitude to National Operational Hydrologic Remote Sensing Center and NOAA for providing climate data. We are very grateful for the help of language editing from Mohamed Freeshah. Two anonymous reviewers are also appreciated for their valuable comments and careful checks. This research was funded by the National Natural Science Foundation of China (Grant No. 41774034), the National Science Fund for Distinguished Young Scholars (Grant No. 41825009) and the Fund for Creative Research Groups of China (Grant No. 41721003).

References

Alonso-Arroyo A, Camps A, Aguasca A, Forte GF, Monerris A, Rudiger C, Walker JP, Park H, Pascual D, Onrubia R (2014) Dual-polarization GNSS-R interference pattern technique for soil moisture mapping. IEEE J Sel Top Appl Earth Obs Remote Sens 7(5):1533–1544

Bilich A, Larson KM (2007) Mapping the GPS multipath environment using the signal-to-noise ratio (SNR). Radio Sci 42(6):1–16

Chew CC, Small EE, Larson KM, Zavorotny VU (2014) Effects of near-surface soil moisture on GPS SNR data: development of a retrieval algorithm for soil moisture. IEEE Trans Geosci Remote Sens 52(1):537–543

China Satellite Navigation Office (2017) BeiDou navigation satellite system signal in space interface control document: Open service signal B1C (version 1.0). Retrieved October 20, 2019, from http://www.beidou.gov.cn/xt/gfxz/201712/P020171226741342013031.pdf

Elósegui P, Davis JL, Jaldehag RTK, Johansson JM, Niell AE, Shapiro II (1995) Geodesy using the global positioning system: the effects

of signal scattering on estimates of site position. J Geophys Res Solid Earth 100(B6):9921–9934
Ester M, Kriegel HP, Sander J, Xu X (1996) A density-based algorithm for discovering clusters in large spatial databases with noise. In: International conference on knowledge discovery and data mining, Portland, Oregon, USA, 2–4 Aug 1996, vol 96(34), pp 226–231
European Union (2016) European GNSS (Galileo) open service signal in space interface control document. OS SIS ICD, Issue 1.3, December 2016
GPS Directorate (2013) Global positioning system modernized civil navigation (CNAV) live-sky broadcast test plan. Global Positioning Systems Directorate, 30 May 2013
Gutmann ED, Larson KM, Williams MW, Nievinski FG, Zavorotny V (2012) Snow measurement by GPS interferometric reflectometry: an evaluation at Niwot Ridge, Colorado. Hydrol Process 26(19):2951–2961
Hauschild A (2017) Combinations of observations. In: Teunissen PJG, Montenbruck O (eds) Springer handbook of global navigation satellite systems. Springer, New York, pp 583–604
Jin S, Qian X, Kutoglu H (2016) Snow depth variations estimated from GPS-reflectometry: a case study in Alaska from L2P SNR data. Remote Sens 8(1):63
Larson KM (2016) GPS interferometric reflectometry: applications to surface soil moisture, snow depth, and vegetation water content in the western United States. Wiley Interdiscip Rev Water 3(6):775–787
Larson KM, Nievinski FG (2013) GPS snow sensing: results from the earthscope plate boundary observatory. GPS Solut 17(1):41–52
Larson KM, Small EE (2014) Normalized microwave reflection index: A vegetation measurement derived from GPS networks. IEEE J Sel Top Appl Earth Obs Remote Sens 7(5):1501–1511
Larson KM, Small EE (2016) Estimation of snow depth using L1 GPS signal-to-noise ratio data. IEEE J Sel Top Appl Earth Obs Remote Sens 9(10):4802–4808
Larson KM, Small EE, Gutmann ED, Bilich AL, Braun JJ, Zavorotny VU (2008a) Use of GPS receivers as a soil moisture network for water cycle studies. Geophys Res Lett 35(24):851–854
Larson KM, Small EE, Gutmann E, Bilich A, Axelrad P, Braun J (2008b) Using GPS multipath to measure soil moisture fluctuations: initial results. GPS Solut 12(3):173–177
Larson KM, Gutmann ED, Zavorotny VU, Braun JJ, Williams MW, Nievinski FG (2009) Can we measure snow depth with GPS receivers? Geophys Res Lett 36(17):1–5
Montenbruck O, Hauschild A, Steigenberger P, Langley RB (2010) Three's the challenge: a close look at GPS SVN62 triple-frequency signal combinations finds carrier-phase variations on the new L5. GPS World 21(8):8–19
Nievinski FG, Larson KM (2014a) Forward modeling of GPS multipath for near-surface reflectometry and positioning applications. GPS Solut 18(2):309–322
Nievinski FG, Larson KM (2014b) An open source GPS multipath simulator in Matlab/Octave. GPS Solut 18(3):473–481
Nievinski FG, Larson KM (2014c) Inverse modeling of GPS multipath for snow depth estimation—part II: application and validation. IEEE Trans Geosci Remote Sens 52(10):6564–6573
Ozeki M, Heki K (2012) GPS snow depth meter with geometry-free linear combinations of carrier phases. J Geod 86(3):209–219
Pan L, Zhang X, Li X, Li X, Lu C, Liu J, Wang Q (2017) Satellite availability and point positioning accuracy evaluation on a global scale for integration of GPS, GLONASS, BeiDou and Galileo. Adv Space Res 63(9):2696–2710
Press WH, Rybicki GB (1989) Fast algorithm for spectral analysis of unevenly sampled data. Astrophys J 338:277–280
Qian X, Jin S (2016) Estimation of snow depth from GLONASS SNR and phase-based multipath reflectometry. IEEE J Sel Top Appl Earth Obs Remote Sens 9(10):4817–4823
Rodriguez-Alvarez N, Bosch-Lluis X, Camps A, Aguasca A, Vall-Llossera M, Valencia E et al (2011) Review of crop growth and soil moisture monitoring from a ground-based instrument implementing the interference pattern GNSS-R technique. Radio Sci 46:1–11
Simsky A (2006) Three's the charm: triple-frequency combinations in future GNSS. Inside GNSS 1(5):38–41
Tabibi S, Nievinski FG, van Dam T, Monico JF (2015) Assessment of modernized GPS L5 SNR for ground-based multipath reflectometry applications. Adv Space Res 55(4):1104–1116
Tabibi S, Geremia-Nievinski F, van Dam T (2017) Statistical comparison and combination of GPS, GLONASS, and multi-GNSS multipath reflectometry applied to snow depth retrieval. IEEE Trans Geosci Remote Sens 55(7):3773–3785
Torrence C, Compo GP (1998) A practical guide to wavelet analysis. Bull Am Meteorol Soc 79(1):61–78
UNAVCO Community (2002) SuomiNet-G GPS Network—SG27-Barrow SuomiNet P.S. UNAVCO, Inc, GPS/GNSS Observations Dataset
Wang X, Zhang Q, Zhang S (2018) Water levels measured with SNR using wavelet decomposition and Lomb–Scargle periodogram. GPS Solut 22(1):22
Yu K, Ban W, Zhang X, Yu X (2015) Snow depth estimation based on multipath phase combination of GPS triple-frequency signals. IEEE Trans Geosci Remote Sens 53(9):5100–5109
Yu K, Li Y, Chang X (2018) Snow depth estimation based on combination of pseudorange and carrier phase of GNSS dual-frequency signals. IEEE Trans Geosci Remote Sens 57(3):1817–1828
Zhang S, Wang X, Zhang Q (2017) Avoiding errors attributable to topography in GPS-IR snow depth retrievals. Adv Space Res 59(6):1663–1669

Mr. Zhiyu Zhang is currently a Master candidate at the School of Geodesy and Geomatics, Wuhan University. He has obtained his B.Sc. at the School of Geological Engineering and Surveying Engineering, Chang'an University, in 2017. His area of research currently focuses on GNSS remote sensing.

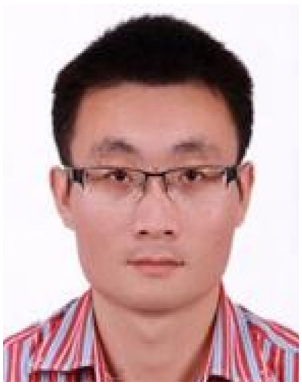

Dr. Fei Guo is currently an associate professor at the School of Geodesy and Geomatics, Wuhan University. He received his B.Sc. degree in Survey Engineering from Nanjing Forestry University in 2007. He obtained his M.Sc. and PhD degrees with distinction in Geodesy from Wuhan University in 2009 and 2013, respectively. His current research mainly focuses on GNSS precise positioning and its application in geoscience.

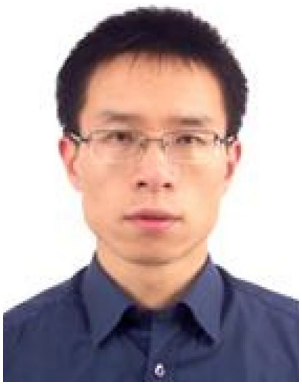

Dr. Xiaohong Zhang is currently a professor at Wuhan University. He obtained his B.Sc., Master, and PhD degrees with distinction in Geodesy and Engineering Surveying at the School of Geodesy and Geomatics at Wuhan University in 1997, 1999, and 2002. His main research interests include precise point positioning (PPP), GNSS/INS navigation, and their applications in geoscience and engineering.